



Contents lists available at ScienceDirect

# Modelling the selective removal of sodium ions from greenhouse irrigation water using membrane technology

Z. Qian<sup>a,c,\*</sup>, H. Miedema<sup>c</sup>, L.C.P.M. de Smet<sup>b,c</sup>, E.J.R. Sudhólder<sup>a</sup><sup>a</sup> Department of Chemical Engineering, Delft University of Technology, Van der Maasweg 9, Delft 2629 HZ, The Netherlands<sup>b</sup> Laboratory of Organic Chemistry, Wageningen University, Stippeneng 4, Wageningen 6708 WE, The Netherlands<sup>c</sup> Wetsus, European Centre of Excellence for Sustainable Water Technology, Oostergoweg 9, Leeuwarden 8911 MA, The Netherlands

## ARTICLE INFO

## Article history:

Received 22 December 2017

Received in revised form 4 March 2018

Accepted 24 March 2018

Available online 9 April 2018

## Keywords:

Greenhouse

Irrigation water

Sodium removal

Mass balance

Modelling

Na<sup>+</sup> over K<sup>+</sup> membrane selectivity

## ABSTRACT

A model is presented for the Na<sup>+</sup> and K<sup>+</sup> levels in the irrigation water of greenhouses, specifically those for the cultivation of tomato. The model, essentially based on mass balances, not only describes the accumulation of Na<sup>+</sup> but includes a membrane unit for the selective removal of Na<sup>+</sup> as well. As determined by the membrane properties, some of the K<sup>+</sup> is removed as well. Based on real-life process parameters, the model calculates the Na<sup>+</sup> and K<sup>+</sup> concentration at three reference points. These process parameters include the evapotranspiration rate, the K<sup>+</sup> uptake by the plants, the Na<sup>+</sup> and K<sup>+</sup> content of the fertilizer, the Na<sup>+</sup> leaching out from the hydroponic substrate material, and the Na<sup>+</sup> and K<sup>+</sup> removal efficiency of the membrane unit. Using these parameters and given a constant K<sup>+</sup> concentration of the irrigation water entering the greenhouse of 6.6 mM (resulting in the optimal K<sup>+</sup> concentration for tomato cultivation), the composition of the solution is completely defined at all three reference points per irrigation cycle. Prime aim of this investigation is to explore the requirements for the selective membrane that currently is developed in our lab. It is found that even for a limited Na<sup>+</sup> over K<sup>+</sup> selectivity of 6, after a number of cycles the Na<sup>+</sup> level reaches steady state at a level below the upper (toxic) threshold for tomato cultivation (20 mM). Economic aspects and ways of implementation of such a system are briefly discussed.

© 2018 The Authors. Published by Elsevier B.V. on behalf of Institution of Chemical Engineers. This is an open access article under the CC BY-NC-ND license (<http://creativecommons.org/licenses/by-nc-nd/4.0/>).

## 1. Introduction

Closed-loop soilless or hydroponic systems are already widely used if not, at least in certain countries e.g. The Netherlands, common practice in horticulture (Sonneveld, 2000). Nutrients and water are supplied continuously to the irrigation water (IW) to compensate for nutrient uptake by the plants and water loss due to evapotranspiration. Ideally, the nutrient and water supply are fine-tuned such that the nutrient con-

centration and the osmotic pressure of the drainage solution remain (fairly) constant. Consequently, nutrients, which are present but are not taken up by the plant, accumulate in the IW. Na<sup>+</sup> is a typical example of an ion that over time builds up in the IW (Qados, 2011). High Na<sup>+</sup> levels inhibit plant growth directly or indirectly by hampering the uptake of other nutrients (Zhang et al., 2010; Blaylock, 1994; Läuchli and Grattan, 2007; Kinraide, 1999). Because of the detrimental effects of high Na<sup>+</sup>, the IW Na<sup>+</sup> level has been subject of numerous studies already (Savvas et al., 2008, 2007; Carmassi et al., 2005). These studies are restricted however to simulation studies, validated or not by mon-

\* Corresponding author at: Wetsus, European Centre of Excellence for Sustainable Water Technology, Oostergoweg 9, Leeuwarden 8911 MA, The Netherlands.

E-mail address: [zexin.qian@wetsus.nl](mailto:zexin.qian@wetsus.nl) (Z. Qian).

<https://doi.org/10.1016/j.cherd.2018.03.040>

0263-8762/© 2018 The Authors. Published by Elsevier B.V. on behalf of Institution of Chemical Engineers. This is an open access article under the CC BY-NC-ND license (<http://creativecommons.org/licenses/by-nc-nd/4.0/>).

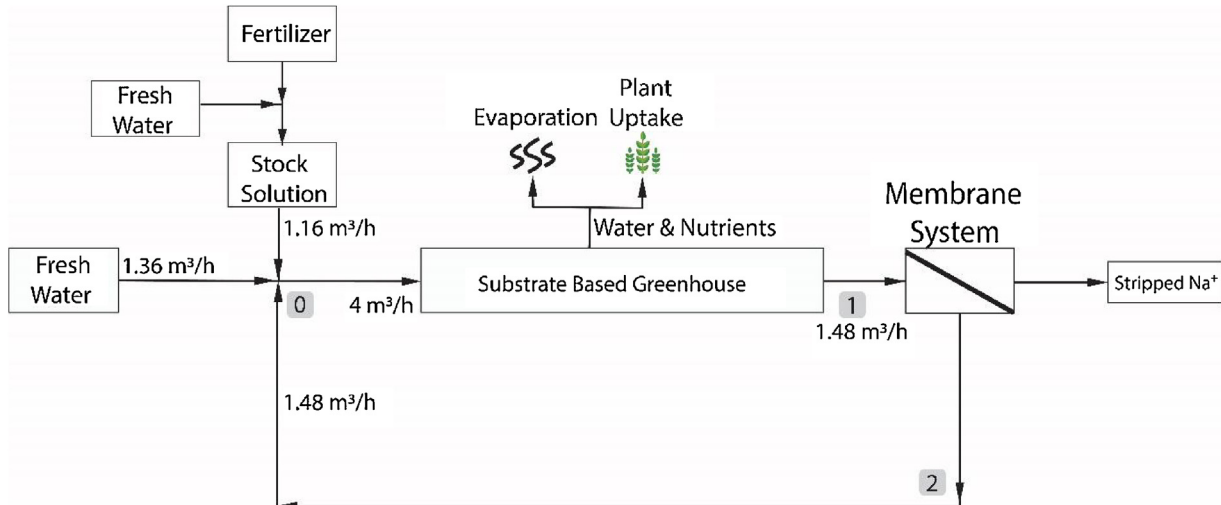


**Fig. 1 – Outline of a substrate-based greenhouse irrigation water system with the drain water recycled and including a membrane unit for the selective removal of  $\text{Na}^+$ . Reference points #0–2 are indicated as well as the relevant (steady-state) volumetric flows while assuming a  $\text{K}^+$  loss of 10% (i.e.,  $\beta = 0.1$ ).**

itoring the actual  $\text{Na}^+$  level in the IW during crop growth. Despite the detrimental effects at higher levels, plants do show a certain tolerance for  $\text{Na}^+$ . Reported  $\text{Na}^+$  threshold values for tomato vary somewhat but levels above 5 dS/m, equivalent to 50 mM, prove to inhibit growth and yield (Zhang et al., 2016). The threshold value might depend on the tomato species; the value used in the present study is 20 mM. As soon as  $\text{Na}^+$  exceeds the threshold level, the IW is discharged and needs to be renewed. After replenishing the system with freshly prepared IW the entire process of  $\text{Na}^+$  building up starts all over again. Our goal is, apart from monitoring, to develop a (membrane-based) system that selectively removes accumulated  $\text{Na}^+$  from the IW. A complication arises from the fact that  $\text{K}^+$ , an essential plant nutrient, has very similar physicochemical properties as  $\text{Na}^+$ . Both (alkali metal) ion species have the same valence (+1) and are similar in size with ionic radii of 1.90 and 2.43 Å for  $\text{Na}^+$  and  $\text{K}^+$ , respectively. However, a key (physiological) difference between the two ion species is that  $\text{Na}^+$  is hardly taken up by the plant and is the major cause of salinity toxicity (Pardo and Quintero, 2002; Maathuis et al., 2014). Excess  $\text{Na}^+$  thus needs to be removed, either by resin-based absorbance technology or membrane technology. The latter is preferred because it circumvents the necessity of resin regeneration once it has become saturated with  $\text{Na}^+$ .

The fact that  $\text{Na}^+$  and  $\text{K}^+$  behave very much the same because they share similar physicochemical properties is exactly the reason that there are no commercial separation membranes available yet that discriminate between the two ion species. Here separation refers to a membrane that allows high fluxes. Selective membranes for ion selective electrodes (ISE) do exist already. However, ion fluxes over such potentiometric membranes are by definition essentially zero (Bobacka et al., 2008; Guinovart et al., 2017). Ceramic NASICON-based membranes do selectively transport  $\text{Na}^+$  (Song et al., 2016). However, only harsh operational conditions like high temperature or high acidity or alkalinity justify their use because of the high price. In addition, the high conductivity demonstrated in battery applications remains relatively low compared to the conductivity of typical polymeric ion exchange membranes (Galama et al., 2016).

To impose selectivity on a polymeric or Liquid Supported Membrane (LSM), a compound is blended in with the membrane polymer or a mobile carrier is added to the organic phase of the LSM (Akieh-Pirkanniemi et al., 2016; Walkowiak and Kozlowski, 2009; Alexandratos and Stine, 2004).  $\text{Na}^+$  selective carriers include natural monensin and the synthetic crown ether 15-crown-5. Monensin has been used for ISE applications as well as for  $\text{Na}^+$  extraction by ionic liquids enriched with monensin (Tohda et al., 1990; Parmentier et al., 2016). Current focus of our lab is on developing a LSM-based system with the organic phase supplemented with 15-crown-5.

The technological challenge thus is to develop a separation membrane that permeates  $\text{Na}^+$  but not, or at least to a much lower extent,  $\text{K}^+$ . Obviously, the less permeable for  $\text{K}^+$ , the less  $\text{K}^+$  needs to be resupplied to compensate for this loss. Therefore, a key question for the membrane-to-be-developed concerns its required  $\text{Na}^+$  over  $\text{K}^+$  permeation selectivity. Crucial here to realize is that there is no need to remove all  $\text{Na}^+$ . Instead, all that needs to be achieved is a (steady-state) concentration of  $\text{Na}^+$  below the threshold for, in this case, tomato cultivation. Apart from the fact that total  $\text{Na}^+$  removal is technologically hardly feasible, it can be expected as a rule of thumb that the higher the membrane selectivity, the higher the investment costs will be. On the other hand, the higher the selectivity the lower the costs for  $\text{K}^+$  re-supply and, even more important, the more sustainable the overall technology. Prime aim of the present study is to explore the required membrane specifications in terms of  $\text{Na}^+$  over  $\text{K}^+$  permeation selectivity and  $\text{K}^+$  and  $\text{Na}^+$  permeability and flux, given real-life operational process parameters (e.g.,  $\text{K}^+$  uptake by tomato, optimal  $\text{K}^+$  level in the IW, evapotranspiration). The simulation study presented here is based on the calculation of the  $\text{K}^+$  and  $\text{Na}^+$  levels at three different reference locations in the IW system and during subsequent cycles of operation. The prime criteria for the optimal membrane characteristics will essentially be based on the largest number of cycles the system can operate continuously at the lowest possible discharge of  $\text{K}^+$ . The membrane specifications resulting from the present analysis will guide us in the currently performed investigation to actually fabricate such a membrane system.

## 2. Material and methods

### 2.1. System and model design

The greenhouse recycling system considered in the present study is schematically shown in Fig. 1. The fresh water source is accumulated rainwater whereas dissolved fertilizer is added as stock solution with a composition adjusted to the requirement of the particular greenhouse crop. Also indicated in Fig. 1 is the membrane unit responsible for  $\text{Na}^+$  removal and producing a waste stream of  $\text{Na}^+$ . Depending on the membrane selectivity, this waste stream is to a more or lesser extent contaminated with  $\text{K}^+$ . Along the process line, three reference points are distinguished: point #0 where fresh water, stock solution and recycled drain water are mixed forming fresh (i.e., next cycle) irrigation water entering the greenhouse; #1 the drain water leaving the greenhouse before it enters the

membrane module and #2 the drain water after filtration by the membrane unit. The model aims to calculate the  $\text{Na}^+$  and  $\text{K}^+$  concentrations during each cycle ( $n$ ) at the three reference points indicated. The nomenclature practiced throughout this study is based on the use of two indices, the first representing the reference point, the second the cycle number. For instance,  $[\text{K}^+]_{2,3}$  refers to the  $\text{K}^+$  concentration at reference point #2 during the third cycle.

## 2.2. Process parameters

The greenhouse crop data used in the simulations were provided by Van der Knaap (The Netherlands) and (the Dutch branch of) Yara International. Van der Knaap exploits greenhouses, cultivating tomatoes; Yara is manufacturer of fertilizer. Taking into account  $\text{K}^+$  uptake by the tomato plants and evapotranspiration, the optimal  $\text{K}^+$  concentration of the IW entering the greenhouse is 6.6 mM whereas the (detrimental) threshold  $\text{Na}^+$  level of the IW in the greenhouse is set at 20 mM.

### 2.2.1. Fertilizer stock solution

Nutrients are added as dissolved salts. The fertilizer stock solution contains 9.5 mM  $\text{K}^+$  and 2.7 mM  $\text{Na}^+$  (Van der Knaap, personal communication).

### 2.2.2. Fresh water

Since rainwater is used as fresh water source at reference point #0, three sets of samples were collected during September–October-2017 at Wetsus in Leeuwarden, the Netherlands. The  $\text{K}^+$  and  $\text{Na}^+$  levels were analyzed using inductively coupled plasma optical emission spectrometry (ICP-OES, Perkin Elmer Optima 5000 Series). All required dilutions were carried out with ultrapure water (Millipore purification unit). The average  $\text{K}^+$  and  $\text{Na}^+$  concentration in rain water was 158  $\mu\text{g/l}$  and 2587  $\mu\text{g/l}$ , resulting in background concentrations of 4  $\mu\text{M}$  and 112.5  $\mu\text{M}$  for  $\text{K}^+$  and  $\text{Na}^+$ , respectively.

### 2.2.3. Water loss (evapotranspiration)

Based on a weekly analysis of their irrigation data, over the year 2016 the average evapotranspiration in the tomato greenhouse of Van der Knaap was 63%, implying the volumetric flow at point #1 (and #2 as well with the assumption of zero water transportation through the membrane during treatment) equals 0.37 times the volumetric flow leaving point #0 and entering the greenhouse.

### 2.2.4. $\text{K}^+$ concentration

$\text{K}^+$  enters the system from two potential sources:

- 1) The background  $\text{K}^+$  concentration in fresh water (4  $\mu\text{M}$ ), and
- 2) The  $\text{K}^+$  content of the fertilizer stream (9.5 mM).

Furthermore,  $\text{K}^+$  leaves the system at two locations. Firstly, the nutritional  $\text{K}^+$  uptake by the crops and, secondly, the loss through the membrane unit due to the given  $\text{Na}^+$  over  $\text{K}^+$  permeation selectivity of the membrane. Given the optimal  $\text{K}^+$  concentration in the IW entering the greenhouse (6.6 mM) and the (fixed) total water loss of 63%, the fraction of added fertilizer at point #0 is adjusted to this value of 6.6 mM. The fraction of  $\text{K}^+$  uptake by the plants ( $\mu$ ) has been determined experimentally by measuring the  $\text{K}^+$  concentrations of the drain water leaving the greenhouse, i.e., at reference point #1. From the

measured value of 11.4 mM and the average concentration of  $\text{K}^+$  entering the greenhouse (6.6 mM):

$$\mu = 1 - \frac{11.4 \times (1 - 0.63)}{6.6} = 0.36$$

### 2.2.5. $\text{Na}^+$ concentration

$\text{Na}^+$  enters the system from three potential sources:

- 1) The background  $\text{Na}^+$  concentration in fresh water (112.5  $\mu\text{M}$ ),
- 2) The  $\text{Na}^+$  content of the fertilizer (2.7 mM), and
- 3) The  $\text{Na}^+$  leaching from the (coconut-based) substrate material used in the greenhouse, leads to a  $\text{Na}^+$  enrichment of the irrigation water (*vide infra*).

Because  $\text{Na}^+$  is not taken up by the plants, it leaves the system only at the membrane unit. At the start of the first irrigation cycle the  $\text{Na}^+$  concentration in the irrigation water is 1.9 mM (resulting from the background  $\text{Na}^+$  concentrations in both fresh water and fertilizer and fixing the  $\text{K}^+$  concentration at point #0 at 6.6 mM). The  $\text{Na}^+$  leaching from the substrate was determined by measuring the  $\text{Na}^+$  concentration at point #1, and found to be 13.5 mM, resulting in a concentration increase (L) of:  $13.5(1 - 0.63) - 1.9 = 3.1 \text{ mM}$ . Even though over time the  $\text{Na}^+$  is washed out the substrate, the present study assumes a constant degree of leaching during the consecutive cycles of operation.

The membrane unit needs to remove  $\text{Na}^+$  to meet a (steady-state)  $\text{Na}^+$  concentration level in the irrigation water <20 mM, i.e., the upper tolerance level for  $\text{Na}^+$  of tomato cultivation. Noteworthy, the model assumes that the membrane unit does not remove any water. The reason is that the LSM under development is composed of a hydrophobic support impregnated with a hydrophobic solvent containing the  $\text{Na}^+$  selective carrier 15-crown-5. Prior to entering this organic phase, ions need to be dehydrated with the free energy ( $\Delta G$ ) of dehydration ( $>0$ ) is compensated for by the  $\Delta G$  of ion coordination by the 15-crown-5( $<0$ ). The water permeation through such LSM systems is negligible.

## 2.3. Mass balances

At the start of each new cycle, the addition of fresh water and fertilizer at reference point #0 has to compensate for the total water loss due to evapotranspiration and  $\text{K}^+$  losses due to plant uptake and removal by the membrane unit. Together with the recycled fraction entering point #0, the fractions of added fresh water and stock solution are adjusted such that the  $\text{K}^+$  concentration of the irrigation water entering the greenhouse at point #0 is 6.6 mM. Given this fixed value of 6.6 mM, adjustment is possible because the total fraction of fresh water and stock solution at point #0 is known to be 1.0 for the first cycle ( $n = 1$ ), and 0.63 for all subsequent cycles ( $n > 1$ ). The calculation of all parameters is thus based on the fraction of fertilizer stock solution ( $\varepsilon$ ) added at point #0. For that reason, we designated  $\varepsilon$  the master variable in our simulations. On the same token,  $\text{K}^+$  is the master ionic species, dictating, by means of  $\varepsilon$ , the concentration of the slave ionic species  $\text{Na}^+$  at point #0 at the start of each new cycle. Once  $\varepsilon$  has been calculated from the mass (or volumetric flow) balance at point #0, the  $\text{Na}^+$  concentration can be calculated as well.

For the very first water cycle, only stock solution and fresh water will meet at point #0. From the second cycle on, however,

**Table 1 – Description of the parameters used throughout this study, corresponding to Figs. 1 and 2.**

Variables	Values
$\Phi_v(1)$	Volumetric flow entering the greenhouse
$\Psi$	$K^+$ concentration in fresh water
X	$Na^+$ concentration in fresh water
N	$K^+$ concentration in fertilizer stock solution
M	$Na^+$ concentration in fertilizer stock solution
$\xi$	Fraction of fresh water added at point #0
$\varepsilon$	Fraction of fertilizer stock solution added at point #0
$\mu$	Fraction of $K^+$ entering the greenhouse taken up by the crop
L	$Na^+$ concentration increase due to $Na^+$ leaching out from the coconut-based substrate
$\theta$	Fraction of $\Phi_v(1)$ lost due to evapotranspiration
$\alpha$	Fraction of $Na^+$ removed from the drain water leaving the greenhouse
$\beta$	Fraction of $K^+$ removed from the drain water leaving the greenhouse
$\gamma$	$Na^+$ over $K^+$ permeation selectivity of the membrane unit

recycled drain water will join these two water streams at point #0. For this reason, the calculation of the first and the following cycles should be considered separately.

### 2.3.1. Volumetric flow balance for the first two cycles

2.3.1.1. First irrigation cycle ( $n = 1$ ). Fig. 2 shows the basic outline of Fig. 1 but complemented with all relevant parameters referred to in this study. Table 1 lists all these parameters as well as their numerical value as used in this study.

Volumetric flows ( $\Phi_v$ ) are presented as fraction of the flow entering the greenhouse,  $\Phi_v(1)$  with  $\varepsilon$  the fraction of the stock solution and  $\xi$  the fraction of fresh water. Flows  $\Phi_v(2)$  and  $\Phi_v(3)$  represent the volumetric flow of fresh water and stock solution added at point #0, respectively.

2.3.1.1.1. Reference point #0. As mentioned, given the optimal  $K^+$  concentration for tomato and taken into account  $K^+$  uptake and evapotranspiration, the  $K^+$  concentration at point #0 is set at 6.6 mM. The  $Na^+$  threshold of 20 mM is the maximum acceptable  $Na^+$  level of the IW leaving the greenhouse. Given the  $Na^+$  leaching out the substrate (3.1 mM) and the evapotranspiration (0.67), the 20 mM translates into a  $Na^+$  of the IW entering the greenhouse of  $20 \times 0.37 - 3.1 = 4.3$  mM. Throughout this study the threshold  $Na^+$  level at point #0 of the incoming IW is set at 4 mM.

The volumetric flow balance reads:

$$\Phi_v(1) = \Phi_v(2) + \Phi_v(3) = \xi_1 \Phi_v(1) + \varepsilon_1 \Phi_v(1) \quad (1)$$

Suppose  $\Psi$  and N are the  $K^+$  concentration in the fresh water and in the fertilizer stock solution, respectively. Then, according to Eq. (1), the  $K^+$  mass balance equals:

$$[K^+]_{0,1} \times \Phi_v(1) = \Psi \times \xi_1 \Phi_v(1) + N \times \varepsilon_1 \Phi_v(1) \quad (2)$$

Because  $\xi_1 + \varepsilon_1 = 1$  and dividing by  $\Phi_v(1)$  renders for the  $K^+$  concentration:

$$[K^+]_{0,1} = (1 - \varepsilon_1)\Psi + \varepsilon_1 N = \varepsilon_1(N - \Psi) + \Psi \quad (3)$$

The fraction of stock solution thus is:

$$\varepsilon_1 = ([K^+]_{0,1} - \Psi)/(N - \Psi) \quad (4)$$

With  $[K^+]_{0,1} = 6.6$  mM and  $\Psi$  and N being known, the value of  $\varepsilon_1$  is defined.

Once  $\varepsilon_1$  is known, the  $Na^+$  concentration for the first cycle can be calculated by:

$$[Na^+]_{0,1} = \xi_1 X + \varepsilon_1 M = \varepsilon_1(M - X) + X \quad (5)$$

where M and X are the  $Na^+$  concentration of the stock solution and fresh water, respectively.

Compared to the  $K^+$  concentration at point #0, the  $K^+$  concentration at point #1 will be different due to  $K^+$  uptake by the plants and evapotranspiration. Because  $[K^+]_{0,n}$  is fixed at 6.6 mM,  $[K^+]_{1,n}$  is directly proportional to  $[K^+]_{0,n}$ . Let  $\mu$  be the fraction of  $K^+$  taken up by the plants and  $\theta$  the fraction of water loss due to evapotranspiration. Then,  $[K^+]_{1,1}$  is given by:

$$[K^+]_{1,1} = [(1 - \mu)[K^+]_{0,1}]/(1 - \Theta) \quad (6)$$

The  $Na^+$  concentration will also change, firstly, because of evapotranspiration, secondly because of the  $Na^+$  that leaches out of the coconut-based substrate used, causing an increase of the  $Na^+$  concentration, represented by L. Then  $[Na^+]_{1,1}$  is given by:

$$[Na^+]_{1,1} = ([Na^+]_{0,1} + L)/(1 - \Theta) \quad (7)$$

2.3.1.1.2. Reference point #2. Reference point #2 is located downstream the membrane unit (permeate side) and calculation of the  $K^+$  and  $Na^+$  concentration at this point therefore requires implementation of the membrane characteristics. Let  $\alpha$  be the fraction of  $Na^+$  (compared to reference point #1) that permeates the membrane (and with that removed from the system) and  $\beta$  the fraction of  $K^+$  that permeates the membrane (also removed from the system). Then the  $K^+$  and  $Na^+$  concentrations are given by  $[K^+]_{2,1} = (1 - \beta)[K^+]_{1,1}$  and  $[Na^+]_{2,1} = (1 - \alpha)[Na^+]_{1,1}$ , respectively.

2.3.1.2. Second irrigation cycle ( $n = 2$ ). The calculations for the second cycle are essentially the same as those for the first cycle. The main difference concerns the starting point, i.e., the volumetric flow balance at point #0, now given by:

$$\Phi_v(1) = \Phi_v(2) + \Phi_v(3) + \Phi_v(5) \quad (8)$$

Expressed in terms of  $\Phi_v(1)$ , Eq. (8) equals:

$$\Phi_v(1) = \xi_2 \Phi_v(1) + \varepsilon_2 \Phi_v(1) + (1 - \Theta) \Phi_v(1) \quad (9)$$

Given  $\xi_2 + \varepsilon_2 + (1 - \Theta) = 1$  and therefore  $\xi_2 = \theta - \varepsilon_2$ , Eq. (9) reads:

$$\phi(v, 1) = (\Theta - \varepsilon_2)\phi(v, 1) + \varepsilon_2\phi(v, 1) + (1 - \Theta)(v, 1) \quad (10)$$

In analogy with Eq. (2), Eq. (10) results in a  $K^+$  concentration and  $\varepsilon_2$  at point #0 of:

$$[K^+]_{0,2} = \xi_2 \Psi + \varepsilon_2 N + (1 - \Theta)[K^+]_{2,1} = (\Theta - \varepsilon_2)\Psi + \varepsilon_2 N + (1 - \Theta)[K^+]_{2,1} \quad (11)$$

$$\varepsilon_2 = ([K^+]_{0,2} - (1 - \Theta)[K^+]_{2,1} - \Theta\Psi)/(N - \Psi) \quad (12)$$

Once  $\varepsilon_2$  has been determined,  $[Na^+]$  at each point can be calculated:

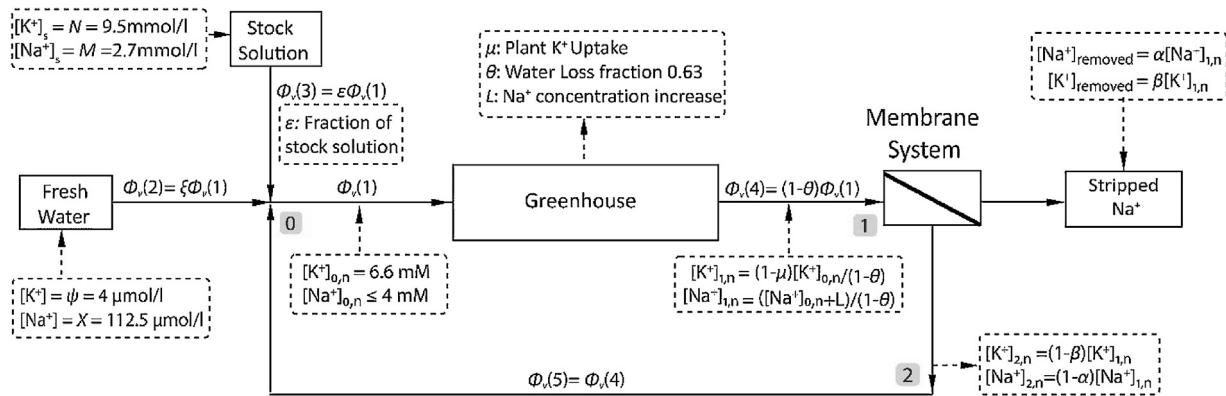


**Fig. 2 – Outline of Fig. 1 complemented with the volumetric flows  $\Phi_v(1)$ – $\Phi_v(5)$  and the process parameters indicated.**

$$[Na^+]_{0,2} = \varepsilon_2(M - X) + \Theta X + (1 - \Theta)[Na^+]_{2,1} \quad (13)$$

$$[Na^+]_{1,2} = \frac{[\varepsilon_2(M - X) + \Theta X] + L}{1 - \Theta} + [Na^+]_{2,1} \quad (14)$$

$$[Na^+]_{2,2} = \frac{(1 - \alpha)}{(1 - \Theta)} [\varepsilon_2(M - X) + \Theta X + L] + (1 - \alpha)[Na^+]_{2,1} \quad (15)$$

Apart from the fact that  $[K^+]_{0,n}$  remains constant for  $n > 1$  (6.6 mM),  $[K^+]_{1,n}$  and  $[K^+]_{2,n}$  are constant as well having (if assuming  $\beta = 0.1$ ) a value of 11.4 and 10.3 mM, respectively. In addition, from the second cycle onwards  $\varepsilon_n$  remains constant as well and independent of  $n$ . This can be seen after, first, substituting  $\varepsilon_1$  into  $[K^+]_{2,1}$  followed by substituting  $[K^+]_{2,1}$  into  $\varepsilon_2$ , resulting in:

$$\varepsilon_n = \frac{[K^+]_{0,n}(1 - (1 - \beta)(1 - \mu)) - \theta \times \Psi}{N - \Psi} \quad (16)$$

According to the parameter values in Table 1,  $\varepsilon_n$  adopts a numerical value expressed in terms of  $\beta$  of  $0.25 + 0.44\beta$  ( $= 0.29$  for  $\beta = 0.1$ ).

### 2.3.2. Generalized expressions

As evident from Eqs. (3)–(5), for the first cycle  $\varepsilon$  and by implication the  $[K^+]$  and  $[Na^+]$  as well can all be expressed exclusively in terms of the known process parameters  $[K^+]_{0,1}$ ,  $\alpha$ ,  $\beta$ ,  $\mu$ ,  $\theta$ ,  $r$ ,  $N$ ,  $M$ ,  $X$  and  $\Psi$ . The same is actually true for the second cycle. This can readily be seen after substituting the expression for  $[Na^+]_{2,1}$  into Eqs. (13)–(15). Because of this, generalized expressions can be derived for  $[Na^+]$  at each reference point as function of known process parameters and the cycle number  $n$ . The advantage of these generalized expressions is that they allow the direct calculation of  $[Na^+]$  during the  $n$ th cycle at each reference point without the need to know (calculate) the concentrations during the previous cycles. As an example but also because Figs. 3 and 4 were constructed using these expressions, the generalized expression for  $[Na^+]_{0,n}$  and  $[Na^+]_{1,n}$  from the 2nd cycle on are given below (for their derivation, see Supplementary information).

$$[Na^+]_{0,n} = (M - X) \sum_{i=1}^n [\varepsilon_i \times (1 - \alpha)^{n-i}] + (X\theta + L) \sum_{i=1}^{n-2} [(1 - \alpha)^i] + (X + L)(1 - \alpha)^{(n-1)} + X\theta \quad (17)$$

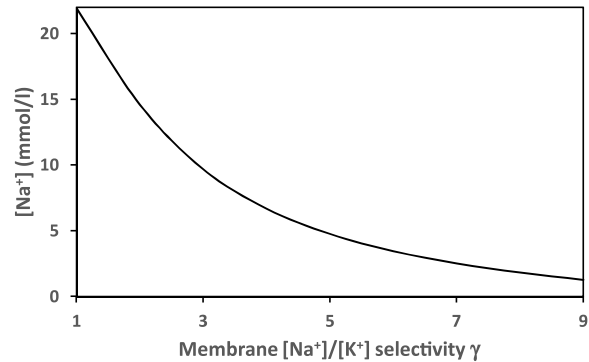


**Fig. 3 – Accumulation of  $Na^+$  in the irrigation water entering the greenhouse (i.e., at point #0) after 10 cycles of operation for a membrane with a  $Na^+/K^+$  selectivity ranging from 1 to 9 and a  $K^+$  permeability  $\beta$  of 0.1, i.e., with 10%–90% of the  $Na^+$  and 10% of the  $K^+$  removed.**

$$[Na^+]_{1,n} = \frac{1}{(1 - \theta)} \left[ \sum_{i=1}^n [\varepsilon_i \times (1 - \alpha)^{n-i}] \right]$$

$$+ [(X\theta + L) \sum_{i=1}^{n-1} (1 - \alpha)^{(i-1)}] + (1 - \alpha)^{(n-1)} \times (X + L) \quad (18)$$

Note that for  $n = 2$  and after a number of repeated substitutions, Eqs. (17) and (18) reduce to Eqs. (13) and (14), respectively.

## 3. Results and discussion

### 3.1. Membrane selectivity

The  $Na^+$  over  $K^+$  permeation selectivity also is an intrinsic membrane property. As stated previously, one of our prime goals is to determine the minimum membrane selectivity ( $\gamma$ ) required to maintain the  $Na^+$  concentration in the IW below the upper tolerance level of 4–5 mM. Because the membrane selectivity ( $\gamma$ ) is defined as the ratio of its permeability towards  $Na^+$  ( $\alpha$ ) and its permeability towards  $K^+$  ( $\beta$ ), the permeation of both ion species is coupled. With both  $\beta$  and  $\gamma$  set at a fixed value,  $\alpha$  can be calculated and with that the  $Na^+$  level at point #2, which, in turn, allows the calculation of the  $Na^+$  level at point #0 at the start of a new cycle.

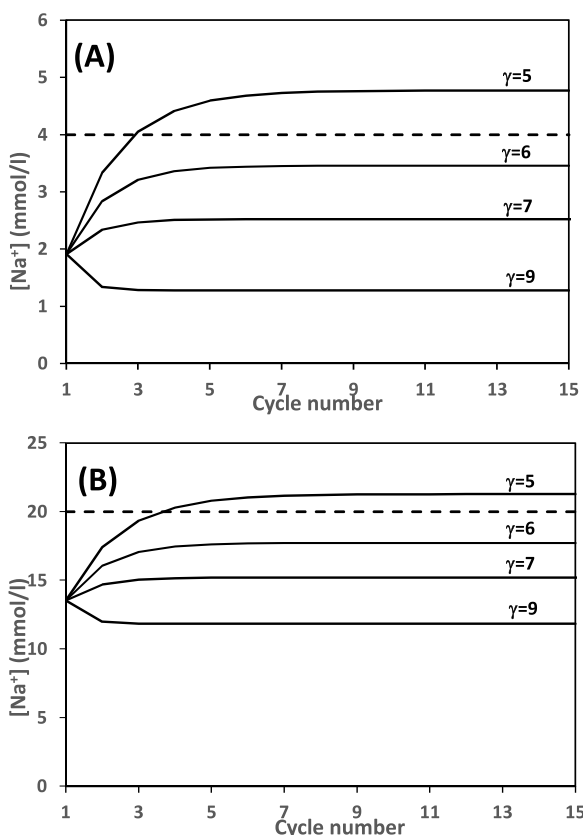


**Fig. 4 – (A) [Na<sup>+</sup>] in the irrigation water entering the greenhouse at point #0; (B) [Na<sup>+</sup>] in the irrigation water leaving the greenhouse at point #1 during 15 cycles of operation, for a Na<sup>+</sup>/K<sup>+</sup> membrane selectivity ranging from 5 to 9 and a K<sup>+</sup> permeability  $\beta$  of 0.1, i.e., with 50%–90% of the Na<sup>+</sup> and 10% of the K<sup>+</sup> removed. Dotted lines represent the threshold of 4 mM of the Na<sup>+</sup> content of the IW entering the greenhouse (A) and the physiological tolerance threshold for tomato of 20 mM (B).**

To compromise between minimizing K<sup>+</sup> loss and dealing with a finite membrane selectivity, the value of  $\beta$  is set (arbitrarily) at 0.1, implying that 10% of K<sup>+</sup> is removed together with Na<sup>+</sup>. In combination with a membrane that does not discriminate between K<sup>+</sup> and Na<sup>+</sup> ( $\gamma = 1$ ) this results in a Na<sup>+</sup> removal of also 10%. In this case it is expected to see a dramatic Na<sup>+</sup> accumulation in the IW. Fig. 3 confirms this expectation showing the Na<sup>+</sup> level in the IW after 10 cycles of operation and for a Na<sup>+</sup> over K<sup>+</sup> selectivity ranging from  $\gamma = 1$  to 9. Note that  $\gamma = 1$  indeed results in staggering Na<sup>+</sup> concentrations after 10 cycles of operation.

Fig. 4 explores the relationship between membrane selectivity and the Na<sup>+</sup> level at points #0 and #1 during 15 subsequent cycles of operation, given the 10% removal of K<sup>+</sup> ( $\beta = 0.1$ ) and for a Na<sup>+</sup> over K<sup>+</sup> membrane permeability selectivity ranging from 5 to 9. A membrane selectivity of 5 does not suffice to achieve a steady-state [Na<sup>+</sup>] below the threshold of 4 mM at point #0 (A) and of 20 mM at point #1 (B). Indeed, it requires at least a selectivity of 6 to accomplish steady-state levels remaining below these thresholds. As indicated in Fig. 2, Na<sup>+</sup> is entering the system from three sources, the fresh water, the fertilizer content and the Na<sup>+</sup> leaching from the coconut-based substrate used. As already remarked, from the second cycle on  $\varepsilon_n$  adopts a constant numerical value of 0.25 + 0.44 $\beta$ , i.e., 0.29 for  $\beta = 0.1$ . Given  $\theta = 0.63$ ,  $\xi$  equals 0.34, implying that the amount of Na<sup>+</sup> entering the system from the fresh water

and fertilizer is 3 and 72 g/h, respectively. The Na<sup>+</sup> concentration increase due to leaching equals 3.1 mM, resulting in 285 g/h. Evidently, at steady state the total amount of 360 g/h equals the amount of Na<sup>+</sup> that needs to be removed by the membrane unit.

In order to maintain a steady-state K<sup>+</sup> concentration in the IW of 6.6 mM, the added amount of K<sup>+</sup>, originating from the fertilizer, equals  $\varepsilon_n \times N \times \Phi_v(1) = 430$  g/h.

### 3.2. Implementation

As argued in the previous paragraph, Na<sup>+</sup> leaching from the substrate contributes most to the amount of Na<sup>+</sup> entering the IW system, even if considering that over time this amount reduces. So even if the Na<sup>+</sup> content of the fertilizer could be drastically reduced, Na<sup>+</sup> still accumulates in the (recycled) IW but at a lower rate.

We envisage implementing the membrane-to-be-developed in an electro dialysis (ED)-like setting, operating under constant current conditions. From the view point of capital costs, a key parameter is the total required membrane surface area (A), given the amount of Na<sup>+</sup> that need to be removed. Eq. (19) gives the value of A as a function of volumetric flow through the membrane module Q, the Faraday constant F (96,485 C/mol), the Na<sup>+</sup> concentration difference between the water entering and leaving the membrane module, the current density (i) and the current utilization factor (f) (Strathmann, 2010):

$$A = Q \times F \times \left( [\text{Na}^+]_{1,2} - [\text{Na}^+]_{2,2} \right) / if \quad (19)$$

The volumetric flow Q equals  $\Phi_v(4) = 0.37 \times \Phi_v(1) = 4.1 \times 10^{-4}$  m<sup>3</sup>/s. As mentioned before, any water flow arising from either osmosis or electro osmosis is ignored, given the strong hydrophobic nature of the LSM system. According to Fig. 2 and given  $\alpha = 0.6$  and  $\beta = 0.1$  (Fig. 4A with  $\gamma = 6$ ),  $[\text{Na}^+]_{0,n}$  reaches a steady-state value of 3.45 mM. The difference between the Na<sup>+</sup> concentration of the solution entering and leaving the membrane then is  $0.6 \times (3.5 + 3.1)/0.37 = 10.7$  mM. Note that this concentration difference results in  $10.7 \times 10^{-3} \times 23 \times 4000 \times 0.37 = 365$  g Na<sup>+</sup>/h that needs to be removed, essentially the same amount as previously derived from the amount of Na<sup>+</sup> entering the system. As for the current density, we take a ‘typical’ value for ion exchange membranes given a total ionic strength of the incoming water of around 25–30 mM, i.e., 10 A/m<sup>2</sup> (Lee et al., 2002). Further, as a rather conservative estimate the current utilization factor (f) is assumed to be 0.6, implying that 60% of the current is actually carried by Na<sup>+</sup>, the remaining 40% by K<sup>+</sup> and other ion species present. Substituting these numbers in Eq. (19) renders a membrane surface area of 70 m<sup>2</sup>. In practice, this could be achieved by constructing ED stacks with a number of cells in series. For instance, three ED modules, each comprising of a stack of 12 cells with a membrane surface area of 2 m<sup>2</sup> each.

So far our analysis has been based on average parameter values over one entire year, thereby ignoring seasonal variations. In any real-life application, the level of evapotranspiration and nutrient uptake will depend on time of the year and crop growth. This asks for a dynamic rather than static nutrient control. One option could be to monitor the water conductivity at point #1 and use this signal as input parameter for the electro dialysis unit. This way, the recorded conduc-

tivity (as measure of the  $\text{Na}^+$  content) allows fine tuning of the constant current magnitude applied during operation, and with that the amount of  $\text{Na}^+$  (and  $\text{K}^+$ ) removed per unit time. Evidently, the implication of such dynamic control is that  $\varepsilon_n$  requires re-adjustment as well.

### 3.3. Economics perspective

The specifications of the membrane-to-be developed, e.g. regarding membrane thickness and the required density of the crown ethers (as carrier molecules) in the membrane, remain elusive and await further study (in progress). Nevertheless, despite these uncertainties a few general remarks can be put forward.

Firstly, the capital cost of the LSM currently developed and validated is to a large extent dominated by the amount of 15-crown-5 needed. When purchased from TCI-Chemicals and given the 15-crown-5 density (0.2 M), the membrane thickness (100  $\mu\text{m}$ ) and a support porosity of 50% the estimated cost price amounts to 78 euro per  $\text{m}^2$ . To put this number in perspective, the price of typical commercially available ion exchange membranes is around 30 euro per  $\text{m}^2$ . The most promising options to bring the price from the LSM down, seem a thinner membrane and upscaling 15-crown-5 (in-house) synthesis. It should be mentioned however that the (at this moment unknown and therefore not considered here) manufacturing cost contribute significantly to if not dominate the cost prize (Fuji Film, Netherlands; personal communication).

Secondly, the operational costs on the other hand will be dominated by the power needed to run the system. Based on the specifications of a typical ED system and given the salt concentration in the feed, the power consumption will be in the range 0.7–2.5 kWh/ $\text{m}^3$  (Al-Karaghoudi and Kazmerski, 2013). The power consumption is linear with the applied current density (Strathmann, 2010) and as evident from Eq. (19), there are essentially three ways to reduce the required total membrane surface area: by reducing the volumetric flow through the system, by increasing the current utilization factor or by increasing the current density. Reduction of the volumetric flow could (possibly) be accomplished by a different configuration altogether. For instance, by positioning the membrane module not in the main stream (as in Figs. 1 and 2) but instead in a bypass. This option will be explored in more detail once we (experimentally) obtained the actual specifications of our membrane under development. Improving the current utilization factor implies a higher  $\text{Na}^+$  over  $\text{K}^+$  membrane selectivity. Even though the cost for re-supplementing the IW with  $\text{K}^+$  will go down, the membrane itself will (probably) be more expensive due to the higher density of crown ethers required. Finally, a higher current density will reduce the total membrane surface area needed but increase the power needed during operation. As pointed out by Strathmann (2010), the opposite effect of current density on required membrane surface area and energy cost may translate in an optimal current density, resulting in the lowest overall costs.

Apart from the foregoing discussion and as remarked earlier on, the prime incentive for the current analysis was inspired more by environmental issues than by economics, even though at a certain point both types of arguments might become intertwined. For instance, (European) legislation becomes more stringent and might even aim for zero discharge in 2027, with discharge allowed only at high(er) cost (European Commission, 2010a, 2010b). For now, it remains

speculative how including such discharge cost will affect the overall balance.

## 4. Conclusion

Excess  $\text{Na}^+$  in irrigation water needs to be removed to a level dictated by the tolerance threshold specific for the particular crop, for tomato 20 mM. The closed-loop irrigation water system described here includes a membrane-based module to remove excess  $\text{Na}^+$  while preserving the (nutrient)  $\text{K}^+$  as much as possible. Based on real-life process parameters, the present study indicates that a  $\text{Na}^+$  over  $\text{K}^+$  membrane permeation selectivity of 6 already suffices to remain the  $\text{Na}^+$  level the plants are exposed to below 20 mM, at least if accepted that 10% of the  $\text{K}^+$  is removed as well. If implemented in an electro dialysis set-up while assuming a constant current density of 10 A/ $\text{m}^2$ , the estimated total membrane surface is 70  $\text{m}^2$ . Considering the opposite effect of current density on required membrane surface area and energy cost, an optimum current density is hypothesized, resulting in a minimum of overall cost.

## Conflict of interest statement

The authors declare that the research was conducted in the absence of any commercial or financial relationships that could be construed as a potential conflict of interest.

## Acknowledgements

This work was performed in the cooperation framework of Wetsus, European Centre of Excellence for Sustainable Water Technology ([www.wetsus.nl](http://www.wetsus.nl)). Wetsus is co-funded by the Dutch Ministry of Economic Affairs and Ministry of Infrastructure and Environment, the European Union Regional Development Fund, the Province of Friesland and the Northern Netherlands Provinces. This work is part of a project that has received funding from the European Union's Horizon 2020 research and innovation programme under the Marie Skłodowska-Curie grant agreement No 65874. The authors like to thank the participants of the research theme "Desalination" for the fruitful discussions and their financial support. A special word of thank goes to Van der Knaap (The Netherlands) and Yara (The Netherlands) for all their advice and providing the necessary greenhouse and fertilizer data. L.C.P.M.d.S. acknowledges the European Research Council (ERC) for a Consolidator Grant, which is part of the European Union's Horizon 2020 research and innovation program (grant agreement No. 682444).

## Appendix A. Supplementary data

Supplementary data associated with this article can be found, in the online version, at <https://doi.org/10.1016/j.cherd.2018.03.040>.

## References

- Akieh-Pirkanniemi, M., Lisak, G., Arroyo, J., Bobacka, J., Ivaska, A., 2016. Tuned ionophore-based bi-membranes for selective transport of target ions. *J. Membr. Sci.* 511, 76–83.
- Al-Karaghoudi, A., Kazmerski, L.L., 2013. Letter to the Editor: energy consumption and water production cost of

- conventional and renewable-energy-powered desalination processes. *Renew. Sustainable Energy Rev.* 24, 343–356.
- Alexandratos, S.D., Stine, C.L., 2004. Synthesis of ion-selective polymer-supported crown ethers: a review. *React. Funct. Polym.* 60, 3–16.
- Blaylock, A.D., 1994. Soil Salinity, Salt Tolerance, and Growth Potential of Horticultural and Landscape Plants. University of Wyoming, Wyoming, p. 4.
- Bobacka, J., Ivaska, A., Lewenstam, A., 2008. Potentiometric ion sensors. *Chem. Rev.* 108 (2), 329–351.
- Carmassi, G., Incrocci, L., Maggini, R., Malorgio, F., Tognoni, F., Pardossi, A., 2005. Modelling salinity build-up in recirculating nutrient solution culture. *J. Plant Nutr.* 28 (3), 431–445.
- European Commission, 2010a. The EU Nitrates Directive, European Union. European Union Publication Office.
- European Commission, 2010b. Water Framework Directive, European Union. European Union Publication Office.
- Galama, A.H., Hoog, N.A., Yntema, D.R., 2016. Method for determining ion exchange membrane resistance for electrodialysis systems. *Desalination* 380, 1–11.
- Guinovart, T., Hernández-Alonso, D., Adriaenssens, L., Blondeau, P., Rius, F.X., Ballester, P., Andrade, F.J., 2017. Characterization of a new ionophore-based ion-selective electrode for the potentiometric determination of creatinine in urine. *Biosens. Bioelectron.* 87, 587–592.
- Kinraide, T.B., 1999. Interactions among  $\text{Ca}^{2+}$ ,  $\text{Na}^+$  and  $\text{K}^+$  in salinity toxicity: quantitative resolution of multiple toxic and ameliorative effects. *J. Exp. Bot.* 50 (338), 1495–1505.
- Läuchli, A., Grattan, S., 2007. Plant growth and development under salinity stress. In: Jenks, M.A., Hasegawa, P.M., Jain, S.M. (Eds.), *Advances in Molecular Breeding Toward Drought and Salt Tolerant Crops*. Springer, Dordrecht, pp. 1–32.
- Lee, H.J., Sarfert, F., Strathmann, H., Moon, S.H., 2002. Designing of an electrodialysis desalination plant. *Desalination* 142 (3), 267–286.
- Maathuis, F.J.M., Ahmad, I., Patishian, J., 2014. Regulation of  $\text{Na}^+$  fluxes in plants. *Front. Plant Sci.* 5, 467–476.
- Pardo, J.M., Quintero, F.J., 2002. Plants and sodium ions: keeping company with the enemy. *Genome Biol.* 3 (6), 1017.1–1017.4.
- Parmentier, D., Lavenas, M., Güler, E., Metz, S.J., Kroon, M.C., 2016. Selective removal of sodium from alkali-metal solutions with tetraoctylammonium monensin. *Desalination* 399, 124–127.
- Qados, A.M.S.A., 2011. Effect of salt stress on plant growth and metabolism of bean plant *Vicia faba* (L.). *J. Saudi Soc. Agric. Sci.* 10 (1), 7–15.
- Savvas, D., Mantzos, N., Barouchas, P.E., Tsirogiannis, I.L., Olympios, C., Passam, H.C., 2007. Modelling salt accumulation by a bean crop grown in a closed hydroponic system in relation to water uptake. *Sci. Hortic.* 111 (4), 311–318.
- Savvas, D., Chatzieustratiou, E., Pervolaraki, G., Gizas, G., Sigrimis, N., 2008. Modelling  $\text{Na}^+$  and  $\text{Cl}^-$  concentrations in the recycling nutrient solution of a closed-cycle pepper cultivation. *Biosyst. Eng.* 99 (2), 282–291.
- Song, S., Duong, H.M., Korsunsky, A.M., Hu, N., Lu, L., 2016. A  $\text{Na}^+$  superionic conductor for room-temperature sodium batteries. *Sci. Rep.* 6, 32330–32339.
- Sonneveld, C., 2000. Effects of salinity on substrate grown vegetables and ornamentals in greenhouse horticulture. In: *ATV Farm Technology*. Wageningen Universiteit, Wageningen, p. 151.
- Strathmann, H., 2010. Electrodialysis, a mature technology with a multitude of new applications. *Desalination* 264 (3), 268–288.
- Tohda, K., Suzuki, K., Kosuge, N., Nagashima, H., Watanabe, K., Inoue, H., Shirai, T., 1990. A sodium ion selective electrode based on a highly lipophilic monensin derivative and its application to the measurement of sodium ion concentrations in serum. *Anal. Sci.* 6, 227–232.
- Walkowiak, W., Kozlowski, C.A., 2009. Macrocycle carriers for separation of metal ions in liquid membrane processes—a review. *Desalination* 240 (1–3), 186–197.
- Zhang, J.L., Flowers, T.J., Wang, S.M., 2010. Mechanisms of sodium uptake by roots of higher plants. *Plant Soil* 326 (1/2), 45–60.
- Zhang, P., Senge, M., Dai, Y., 2016. Effects of salinity stress on growth, yield, fruit quality and water use efficiency of tomato under hydroponic system. *Rev. Agric. Sci.* 4, 46–55.